ORGANIZATION OF CALCIUM PUMP PROTEIN DIMERS IN THE ISOLATED SARCOPLASMIC RETICULUM MEMBRANE

C. A. NAPOLITANO
Cardiology Division, Department of Medicine, University of Connecticut, Farmington, Connecticut 06032

P. COOKE
Department of Physiology, University of Connecticut, Farmington, Connecticut, 06032

K. SEGALMAN
Franklin and Marshall College, Lancaster, Pennsylvania 17604

L. HERBETTE
Cardiology Division, Department of Medicine, University of Connecticut, Farmington, Connecticut 06032

ABSTRACT The arrangement of the calcium pump protein in the isolated sarcoplasmic reticulum (SR) membrane was examined by optical diffraction of freeze-fracture electron micrographs. Several states of protein particle organization were observed: random, hexagonal and tetragonal packing, and a mixture of hexagonal and tetragonal packing. This suggests that the time-averaged positions of protein particles in the plane of the SR membrane are weakly defined. In addition, there appears to be a greater degree of local or short-range order compared to long-range order within the field of freeze-fracture particles. We utilized measurements from tetragonally or hexagonally packed arrays to determine a unit cell area occupied by each freeze-fracture particle and its associated lipid matrix. When these unit cell areas and the stereologically determined area per freeze-fracture particle were compared to the cross-sectional area occupied by a single calcium pump protein and its associated lipid, obtained by x-ray and neutron diffraction methods, we concluded that each freeze-fracture particle probably represents a dimer of pump protein molecules in the plane of the SR membrane.

INTRODUCTION

The sarcoplasmic reticulum (SR) membrane of skeletal muscle is a continuous system of membranous tubules that extends throughout the sarcoplasm and forms a close-meshed canalicular network around each myofibril. The SR releases ionized calcium to initiate muscle contraction, and sequesters the calcium ions to cause relaxation. Calcium sequestration is an active process that is carried out by an ATP-dependent calcium pump protein (1, 2). Studies of the molecular structure of isolated SR membrane vesicles, utilizing low angle lamellar x-ray diffraction (3–6), have shown that the calcium pump protein spans the lipid bilayer with a substantial portion of its mass protruding into the extravesicular space (7). Equatorial x-ray diffraction (3, 4) has provided minimal information as to the distribution of the calcium pump protein in the plane of the SR membrane but this information has contributed to the current model that depicts the arrangement of the calcium pump protein to be liquidlike at temperatures above 5° C (7, 8). Electron micrographs of freeze-fractured SR vesicles show concave and convex fracture surfaces that represent the outer and the inner faces of the membrane bilayer, respectively (9). The outer concave face is characterized by the presence of 75–90 Å particles (9, 10), whereas the inner convex face is generally devoid of such structures (Fig. 1). These intramembranous particles are thought to represent either monomers or oligomers of the calcium pump protein, but the precise number of protein molecules per freeze-fracture particle is yet unresolved (11).

We have studied the in-plane protein organization and freeze-fracture particle composition of the SR by examining electron micrographs of freeze-fractured SR vesicles with optical diffractometry. Our observations indicate that the calcium pump protein is not always distributed randomly in freeze-fracture micrographs of the SR membrane, but may be weakly packed in hexagonal or tetra-

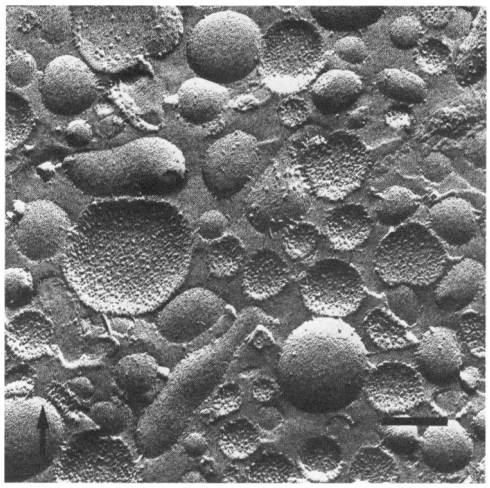

FIGURE 1 Electron micrograph of freeze-fractured SR vesicles. Outer (concave) fracture faces contain many intramembraneous particles that are generally absent from the inner (convex) fracture faces. A 6-s application of platinum and carbon at an angle of 50° produced a platinum and carbon shadow thickness of ~100 Å and 200 Å, respectively. An arrow indicates the shadow direction. Calibration bar = 0.1 μm.

gonal arrays. We conclude, based on the calculated unit cell areas of the hexagonal and tetragonal arrays and a direct evaluation of the average cross-sectional area of a single calcium pump protein molecule within the hydrocarbon core of the SR membrane (5, 7, 12), that two pump protein molecules form a complex for each freeze-fracture particle.

MATERIALS AND METHODS

Membrane Preparation

SR membrane vesicles were prepared from white muscle of rabbit hind limb by homogenization and differential centrifugation (13, 14). Further purification was then carried out on a discontinuous (step) gradient as the fraction sedimenting between 28 and 31% sucrose was collected (15, 16). Protein concentration was determined by the method of Lowry et al. (17) using bovine serum albumin as standard. Total phospholipid content was determined by the method of Chen et al. (18), a procedure that assays inorganic phosphorus.

Freeze Fracture/Electron Microscopy

Samples for freeze fracture were prepared by suspending 1-mg protein of pelleted SR vesicles in 20% (wt/wt) glycerol solution for 2 h at 4° C. The pellets were then placed in gold alloy specimen carriers and quick-frozen in liquid freon cooled by liquid nitrogen. Specimens were freeze fractured at −100° C and deep-etched at −100° C on a Balzers B360M freeze-etching apparatus (Balzers High Vacuum Corp., Santa Anna, CA). A 6 s application of platinum and carbon at an angle of 50° produced a platinum and carbon shadow thickness of ~100 and 200 Å, respectively. This relatively high shadow angle was chosen to reduce the degree of cast shadow in our micrographs. The replicas were floated off onto distilled water, cleaned with 5% Clorox, and picked up on electron microscope grids. Grids were examined in a Hitachi HU11E electron microscope (Hitachi, Ltd., Tokyo, Japan) with an accelerating voltage of 75 kV. A typical micrograph is shown in Fig. 1.

Stereological Procedure

The freeze-fracture electron micrographs (magnification of 49,000) of the two-fracture faces of SR vesicles were photographically enlarged (5.3 times) to facilitate the identification of the intramembranous particles in the evaluation of particle density and in the construction of optical masks. For the stereological analysis of the concave (outer) fracture faces, a small circle of known area was randomly applied to these concave profiles and the particle number within this area was determined (19). Only intramembranous particles with diameters of 75–80 Å located within ~0.9 radii of the center of the vesicle were considered in the analysis.

Three methods were employed in the stereological determination of the area occupied per particle.

Method I. A test circle of 180-Å radius was applied to a concave profile a specified number of times as defined by the diameter of the vesicle (Table I) and the average number of particles per area was determined. For each application of the test circle, a particle count was taken twice using different criteria for counting particles. In the first count, a particle was counted only when it was entirely within the test circle; the second count included any portion of a particle within the test circle. The calculated values of $Å^2$/particle determined from each set of data are presented as an average in Table II.

Method II. A test circle of 180-Å radius was used as described in Method I. For each application of the test circle a particle was counted only when at least 50% of the particle mass was within the test circle.

Method III. One of three test circles of various radii (Table I) was applied to a concave profile and particle density was determined based on the number of particles with 50% or more of their mass within the test circle. This method attempted to match the size of the test circle with the size of the vesicle being examined.

Optical Diffraction

Optical diffraction analysis of electron micrographs is complicated by irregularities in the electron micrograph. In the case of electron micrographs of freeze-fractured SR vesicles, particle distortion from platinum shadowing would negate their direct use as an optical mask. To overcome this problem, the enlarged photographs of the freeze-fracture electron micrographs of SR vesicles were examined as follows. The central portion of the concave fracture plane was chosen to minimize the spacial distortion of particles due to the extreme curvature of the fracture face edge. An optical dot mask was then prepared by overlaying a plastic transparent sheet onto the enlarged photograph and marking the location of each particle with a dot of India ink that approximated the size of the freeze-fracture particle. Because the freeze-fracture particle size (75–90

TABLE I
CRITERIA EMPLOYED IN THE STEREOLOGICAL ANALYSIS OF SARCOPLASMIC RETICULUM VESICLES VIA METHODS I, II, AND III

Vesicle population	Fracture face diameter	Number of test circle* applications (method I, II)	Test circle radius (method III)
	Å		Å
A	800–1,500	1	180
B	1,500–2,300	2	250
C	2,300–3,100	3	375

*Radius = 180 Å.

TABLE II
STEREOLOGICAL ANALYSIS OF THREE POPULATIONS OF CONCAVE FRACTURE FACES FROM FREEZE-FRACTURE ELECTRON MICROGRAPHS OF SARCOPLASMIC RETICULUM UTILIZING THREE ANALYTICAL METHODS

Vesicle population	n	Method		
		I	II	III
			$Å^2$/particle	
A	65	9,800 ± 300	11,300 ± 200	11,300 ± 200
B	31	9,700 ± 300	11,300 ± 300	11,600 ± 400
C	4	10,000 ± 400	11,500 ± 400	13,600 ± 900
Total	100	9,800 ± 200	11,300 ± 200	11,500 ± 200

Each entry is a mean ± SEM.

Å) is comparable to the average nearest neighbor separation (90–120 Å) (20, 21) in freeze-fracture micrographs of SR, potential scattering from the particle shape would obscure the low-angle diffraction arising from the particle distribution. The contribution of this large circular aperture arising from the dot was convoluted out of the diffraction patterns by reducing dot patterns to point patterns. The points corresponded to the center of each particle in the freeze-fracture micrographs and thus preserved the spatial distribution of the protein particles in the membrane plane. These point patterns, which typically contained 30 to 100 particles (mean ± SEM: 62 ± 4) from a single fracture face, were then photographically reduced (7.2 times) onto negative film (Kodalith Ortho film; Eastman Kodak Co., Rochester, NY). The high contrast masks were mounted in an optical diffractometer (Oriel Corp. of America, Stamford, CT) and diffraction patterns were recorded onto Polaroid Type 55 film (Polaroid Corp., Cambridge, MA). The diffractometer was equipped with a helium-neon gas laser (3 mW) and utilized a beam expander and spatial filter assembly with an output focusing lens to recollimate the beam.

Diffraction patterns from point-optical masks revealed the random or weak lattice arrangements for the particles in the freeze-fracture micrograph. The spatial arrangement of the freeze-fracture particles was somewhat obscured when diffraction from a dot pattern was attempted. Such diffraction patterns showed that scattering from the particle shape dominated the optical transform (20). In this case, the particle shape is a circular aperture of radius a with the intensity, $I \propto J_1(\Pi au)/(\Pi au)$, where u is a radial coordinate and J_1 is a first-order Bessel function. This would lead to the erroneous conclusion that the particle organization was random. Because we were interested in the spatial arrangement of the freeze-fracture particles, our point mask approach is justified.

RESULTS AND DISCUSSION

Particle Density

The stereological analysis of the concave profiles of SR vesicles is presented in Table II. The results of the three methods used in the determination of particle density and hence the area per particle are in reasonable agreement. Our range of 10,000–12,000 $Å^2$ for the area occupied by a freeze-fracture particle is lower than other published stereological examinations of the SR membrane in freeze fracture (20, 21).

Particle Organization

The use of optical diffraction for image analysis of electron micrographs was first employed by Klug and Berger to analyze negatively stained biological molecules (22). Its primary value in image analysis lies in the identification and interpretation of organizational features in the electron micrograph specimens that are not immediately apparent to the eye but clearly evident in the optical transform. Each diffraction maximum corresponds to a direction in which a regular periodicity occurs in the optical mask, while the distance of the diffraction maximum from the origin is inversely related to the spacing of the diffracting structures. Therefore in freeze-fractured SR vesicles both short- and long-range particle organization and the average interparticle separation can be determined.

Fig. 2 shows low-angle diffraction patterns of optical masks prepared from freeze-fractured SR vesicles. The diffraction patterns of several concave fracture faces of SR vesicles (n = 50) indicate the existence of several states of particle organization: (*a*) random packing, (*b*) hexagonal packing, (*c*) tetragonal packing, and (*d*) a mixture of

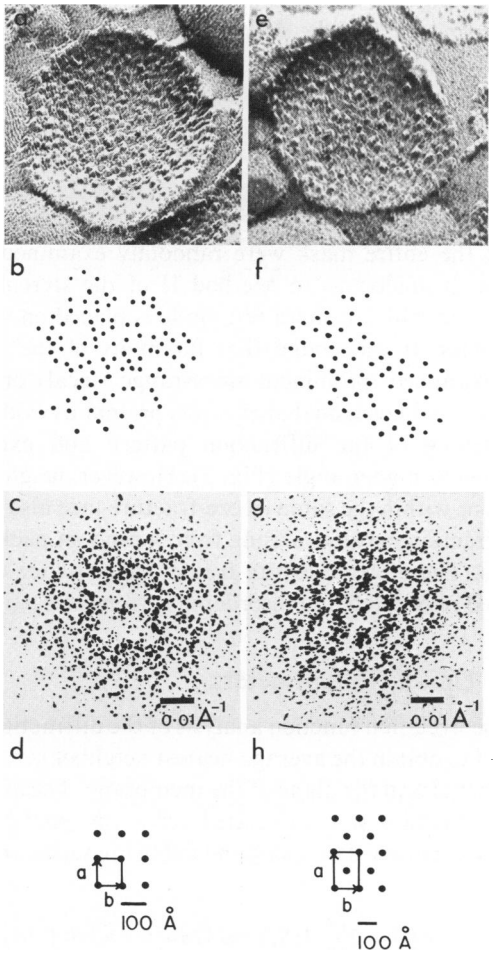

FIGURE 2 Illustration of the relationship between the concave fracture face of an SR vesicle (*a*, *e*), the representative dot (or point) pattern (*b*, *f*), the low-angle optical diffraction pattern (*c*, *g*), and the unit cell dimensions in real space coordinates (*d*, *h*) from a tetragonally packed (*a–d*) and a hexagonally packed (*e–h*) array of freeze-fracture particles in the plane of the SR membrane.

hexagonal and tetragonal packing. Examples of diffraction from tetragonally and hexagonally packed arrays are shown in Fig. 2.

Long-range ordering of freeze-fracture particles was examined effectively using the criteria of Method III described for the stereological studies. Thus, the size of the optical mask was in proportion to the size of the vesicle being examined as shown in Fig. 2. Diffraction patterns indicative of a random arrangement of protein particles and characteristic of scattering from a monotomic liquid were observed in 11% of the diffraction patterns. Approximately 24% of the diffraction patterns demonstrated a tetragonal packing of particles that was characteristic of a tetragonal lattice with random displacement about each lattice point. Hexagonal packing was observed for 15% of the diffraction patterns but a considerable degree of disorder about each lattice point was again evident. The absence of long-range order was observed in many of these patterns indicating a paracrystalline nature for the packing of the protein molecules in the plane of the SR membrane (23). The long-range particle organization can best be described as weak, since half of the diffraction patterns appear to be the result of an intermediate organization with both tetragonal and hexagonal packing characteristics.

The weak long-range ordering of the freeze-fracture particles in the plane of the SR membrane is contrasted by a stronger short-range organization. The laser beam was focused to intersect ~25% of an optical mask and subregions of the entire mask were randomly examined. This operation is analogous to Method II of the stereological procedure in which a small test circle is placed on various size vesicles. It was found that for many of the optical masks examined, prominent short-range (local) order of tetragonal and hexagonal arrays was present as evident by a sharpening of the diffraction pattern and extensive diffraction at higher angle (Fig. 3). However, neighboring subregions within the same freeze-fracture face also exhibited diffraction patterns arising from a random packing of particles. Therefore an entire freeze-fracture face can be composed of ordered and disordered regions of particles.

Unit Cell Parameters

An autocorrelation function analysis of the diffraction data was used to obtain the average nearest neighbor separation of the particles in the plane of the membrane. The autocorrelation function was calculated from the background-corrected intensity data using the following series approximation

$$A(a_j \text{ or } b_j) = 2\sum_{k=0}^{N_k} I(S_k) \cos [2\pi a_j \text{ (or } b_j) S_k] \Delta S;$$

$$a_j = j \Delta a;\ b_j = j \Delta b;\ S_k = k \Delta s;$$

$$\Delta a = \Delta b = 1 \text{ Å};\ \Delta s = 1/22356 \text{ Å};$$

N_k = total number of data points.

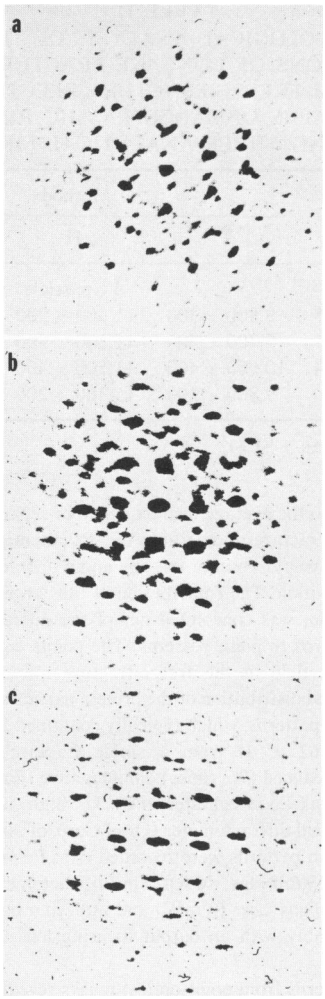

FIGURE 3 Optical diffraction patterns from subregions of different point masks. Prominent short-range ordering of the freeze-fracture particles in the plane of the SR membrane is indicated by these diffraction patterns of hexagonally (*a*) and tetragonally (*b*, *c*) packed arrays. Note the sharpness of these patterns compared to those shown in Fig. 2.

The interval Δs is sufficiently small that $I(s)$ is approximately constant within Δs, and therefore the above equation closely approximates $A(a_j \text{ or } b_j) = F^{-1}[I(s)]$, where F^{-1} is the Fourier transform operator. This autocorrelation analysis provides a value of the unit cell dimension, *d*, from its pseudoperiodicity. For the tetragonal array the unit cell dimensions are equal to 117 ± 7 Å in the *a* direction and 105 ± 5 Å in the *b* direction (Fig. 2 *d*) yielding a unit cell area of 12,285 Å^2 per freeze-fracture particle. The hexagonal array can best be described by a rectangular unit cell (Fig. 2 *h*) as found for the packing of cytochrome c oxidase by Frey et al. (24). The layer line repeat of the hexagonal array of 131 ± 2 Å yields a unit cell area per freeze-fracture particle of 12,969 Å^2 (25,938 Å^2:2 freeze-fracture particles) consistent with that obtained for the tetragonal array.

The models in Fig. 4 illustrate that slight variations in the positions of a random particle arrangement can result

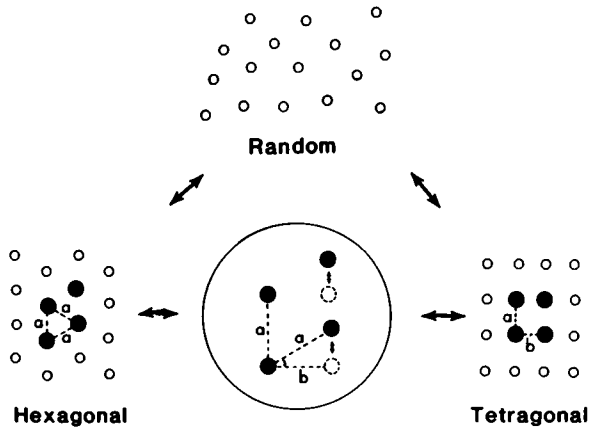

FIGURE 4 Model representation of the organization of the freeze-fracture particles in the concave fracture face of the SR membrane. The models illustrate how variations in the positions of a random particle arrangement can result in either a hexagonal or a tetragonal lattice; (*inset*) a net change in alternate columns of particles can transform a tetragonal array into a hexagonal arrangement, or vice versa. The optical diffraction data indicate that the freeze-fracture protein particles are organized predominantly into hexagonal or tetragonal arrays, although some diffraction patterns are indicative of a liquidlike (random) organization of the freeze-fracture particles.

in either a hexagonal or tetragonal array orientation; as an example, a net change in alternate columns of particles can transform a tetragonal array into a hexagonal arrangements, or vice versa. Pringle (25) has shown that it is possible to transform an almost square lattice into a hexagonal lattice by equal displacement of all the lattice points. Such a model, in which lateral diffusion of membrane protein and phospholipids could be responsible for transitions in the calcium pump protein organization, is plausible in view of the fluid nature of the SR membrane. The freeze-fractured SR vesicles may therefore represent different organizational states when the SR membrane is frozen instantaneously.

Calcium Pump Protein/Freeze-Fracture Particle Comparison

Optical diffraction analysis of SR freeze fracture can represent an important tool when used in conjunction with other independent structural approaches. Our findings regarding the average nearest neighbor particle separation in freeze-fracture micrographs of SR vesicles are consistent with our recent measurements of the size of the calcium pump protein determined by x-ray and neutron diffraction studies (5, 7, 12). The average diameter of a single calcium pump protein within the hydrocarbon core of the SR lipid bilayer, excluding the extravesicular protein knob, was determined to be 55 ± 2 Å, which corresponds to an average cross-sectional area of 2,375 ± 130 Å^2 (5, 7, 12). We emphasize that the overall average diameter of the calcium pump protein molecule including the extravesicular proteinaceous knob may be different from the average diameter within the hydrocarbon core (5, 7, 12, 26) depending upon the packing constraints of the rather large protein knob at the extravesicular surface of the SR membrane. The finding of Dupont et al. (3) and Worthington and Liu (4) regarding the broad and diffuse 55-Å equatorial maxima in their x-ray diffraction patterns suggests that the calcium pump protein may best be described as a cylinder of 60–65-Å diameter within the SR membrane. These data are consistent with our results regarding the overall size of the pump protein within the SR membrane. Because freeze fracture probes the intramembrane region of membranes, we must utilize that structural information regarding the size of the pump protein only within the hydrocarbon core of the SR membrane.

In our micrographs, freeze-fracture particles (75–80 Å) have an average cross-sectional area of ~4,660 Å^2 as compared to the average cross-sectional area of a single pump protein molecule (2,375 ± 130 Å^2) suggesting that each freeze-fracture particle is a dimer of calcium pump protein molecules. Since freeze-fracture particle size is not necessarily a good estimate of protein size because of the possible overestimation caused by shadow artefact or annular lipid, a more accurate comparison is that of the unit cell areas. Our optical diffraction measurements of the hexagonal or tetragonal array parameters indicate a unit cell area per freeze-fracture particle of ~12,000–13,000 Å^2. Our stereological studies showed that the area per freeze-fracture particle was ~10,000–12,000 Å^2. This area corresponds to the area occupied by one freeze-fracture particle and its associated membrane lipid area. X-ray and neutron diffraction measurements indicate that one calcium pump protein molecule plus its associated lipid occupy an area of ~5,800 Å^2.[1] If we assume the area per freeze-fracture particle to be 12,000 Å^2, a value of ~2.1 protein monomers per freeze-fracture particle is obtained.

These stereological and optical diffraction studies utilized concave fracture planes because these surfaces contain the majority of the freeze-fracture particles. Wang et al. (21) have reported that ~10% of the particles observed in freeze fracture can reside on the convex fracture surface, while we estimate that <10% of the particles are located on this surface. However, if we correct our particle distribution for this 10% underestimation as observed by Wang et al. (21), our area per freeze-fracture particle would decrease due to an increase in our observed particle

[1]The lipid to protein ratio is 113 ± 6 (mean ±SEM) moles of phospholipid per mole of protein in this fraction of SR. Therefore, ~57 phospholipid molecules with an average cross-sectional area of 60 Å^2 per phospholipid reside in each monolayer of the SR lipid bilayer. One calcium pump protein (2,375 Å^2) plus its associated lipid occupy an area of ~5,795 Å^2. Because our x-ray, neutron, and optical diffraction studies utilized the same highly purified SR fraction, the observed lipid to protein ratio range used in the calculation of unit cell area does not represent a major source of error.

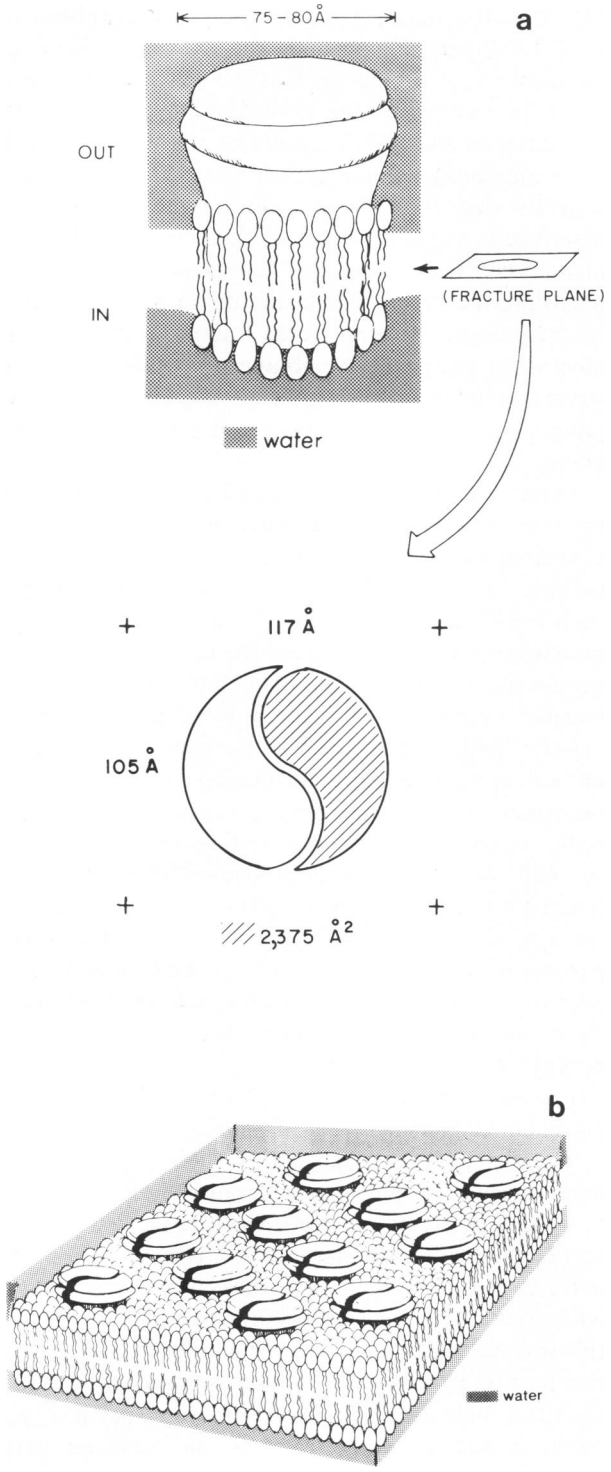

FIGURE 5 (*a*) Schematic representation of a cross-sectional slice through a freeze-fracture particle at the fracture surface depicting two calcium pump protein monomers within the unit cell of dimensions 105 Å × 117 Å for a tetragonal array. (*b*) Schematic representation of the calcium pump protein complex organized in a hexagonal array in the plane of the SR membrane bilayer with each particle complex portrayed as a dimer of pump protein molecules. Some of the structural detail shown in these models regarding the protein knob, which protrudes above the plane of the phospholipid bilayer, and the location of water in the SR membrane was obtained from x-ray and neutron diffraction studies (5, 7, 12).

density, and the above calculation would yield 2.0 protein monomers per freeze-fracture particle. These structural findings regarding the potential organization of pump protein dimers in the SR membrane plane are consonant with several studies that conclude that the functional unit for active calcium transport is a dimer of pump protein molecules (21, 27–29).

A comparison of the intramembranous particles of freeze fracture and the 40-Å surface particles of negative staining in terms of their particle organization is complex due to the physical nature of these structures. Comparisons of freeze-fracture particles, which represent the calcium pump protein in the plane of the SR bilayer, to surface particles of negatively stained SR, which may represent protein subunits penetrating the SR membrane, have indicated that the density of surface particles is greater than that of the intramembranous particles (11, 20). A relative ratio of 3–4:1 for surface to intramembranous particles reported by other investigators (20, 30) for rabbit skeletal SR, and our determination that each freeze-fracture particle is a dimer of calcium pump protein molecules would indicate that ~2 surface particles may represent a pump protein monomer.

Optical diffraction analysis of freeze-fracture may be complicated by lipid phase separation and protein aggregation at lower temperatures (31). The particle organization we have found in freeze-fracture electron micrographs of unfixed SR preparations has not been described in freeze-fracture replicas of intact SR from fixed whole muscle (32–38). However, these studies did not directly test for particle organization as we have in isolated SR fracture faces. It is therefore possible that local ordering of freeze-fracture particles also exists in whole muscle. Further biophysical investigations of whole muscle and isolated SR preparations may resolve this issue and provide a high resolution structural model for the active transport and release of calcium by the sarcoplasmic reticulum membrane (Figs. 5, *a* and *b*).

The authors thank Dr. H. Takenaka for valuable suggestions in the interpretation of these findings, and Dr. Arnold M. Katz for advice regarding the manuscript.

This work was supported by research grants HL-27630, HL-22135, HL-26903, HL-21812, and HL-00911 from the National Institutes of Health (NIH) and by an established investigatorship of the American Heart Association to Dr. Cooke. Dr. Napolitano is supported by NIH training grant HL-07420.

Received for publication 7 June 1982 and in final form 10 December 1982.

REFERENCES

1. Ebashi, S., and F. J. Lipmann. 1962. Adenosine triphosphatase-linked concentration of calcium ions in a particulate fraction of rabbit muscle. *J. Cell. Biol.* 14:389–400.
2. Hasselbach, W., and M. Makinose. 1961. Die Calciumpumpe der "Erschlaffungsgrana" des Muskels und ihre Abhängigkeit von der ATP-Spaltung. *Biochem. Z.* 333:518–528.

3. Dupont, Y., S. C. Harrison, and W. Hasselbach. 1973. Molecular organization in the sarcoplasmic reticulum membrane studied by x-ray diffraction. *Nature (Lond.)*. 244:555–558.
4. Worthington, C. R., and S. C. Liu. 1973. Structure of sarcoplasmic reticulum membranes at low resolution (17 Å). *Arch. Biochem. Biophys.* 157:573–579.
5. Herbette, L., J. Marquardt, A. Scarpa, and J. K. Blasie. 1977. A direct analysis of lamellar x-ray diffraction from hydrated oriented multilayers of fully functional sarcoplasmic reticulum. *Biophys. J.* 20:245–272.
6. Herbette, L., A. Scarpa, J. K. Blasie, C. T. Want, A. Saito, and S. Fleischer. 1981. Comparison of the profile structures of isolated and reconstituted sarcoplasmic reticulum membranes. *Biophys. J.* 36:47–72.
7. Herbette, L. 1980. Structure-function correlation studies of isolated and reconstituted sarcoplasmic reticulum membranes. Ph.D. Dissertation, University of Pennsylvania, Philadelphia, PA.
8. Davis, D. G., G. Inesi, and T. Gulik-Krzywicki. 1976. Lipid molecular motion and enzyme activity in sarcoplasmic reticulum membrane. *Biochemistry*. 15:1271–1276.
9. Baskin, R. J., and D. W. Deamer. 1969. Ultrastructure of sarcoplasmic reticulum preparations. *J. Cell. Biol.* 42:296–307.
10. Tillack, T. M., R. Boland, and A. Martonosi. 1974. The ultrastructure of developing sarcoplasmic reticulum. *J. Biol. Chem.* 249:624–633.
11. Jilka, R. L., A. Martonosi, and T. W. Tillack. 1975. Effect of the purified (Mg^{2+} + Ca^{2+})-activated ATPase of sarcoplasmic reticulum upon the passive Ca^{2+}-permeability and ultrastructure of phospholipid vesicles. *J. Biol. Chem.* 250:7511–7524.
12. Blasie, J. K., J. M. Pachence, and L. Herbette. 1983. Comment on the importance of appropriate neutron diffraction data in the decomposition of membrane scattering profiles into the separate scattering profiles of their molecular components. *In* Neutrons in Biology (Brookhaven Symp.) B. Schoenborn, editor. Plenum Press, New York.
13. Harigaya, S., and A. Schwartz. 1969. Rate of calcium binding and uptake in normal animal and failing human cardiac muscle: membrane vesicles (relaxing system) and mitochondria. *Circ. Res.* 25:781–794.
14. Katz, A. M., D. I. Repke, and W. Hasselbach. 1977. Dependence of ionophore- and caffeine-induced calcium release from sarcoplasmic reticulum vesicles on external and internal calcium ion concentrations. *J. Biol. Chem.* 252:1938–1949.
15. Meissner, G. 1975. Isolation and characterization of two types of sarcoplasmic reticulum vesicles. *Biochim. Biophys. Acta.* 389:51–68.
16. Caswell, A. H., Y. H. Lau, and J.-P. Brunschwig. 1976. Ouabain-binding vesicles from skeletal muscle. *Arch. Biochem. Biophys.* 176:417–430.
17. Lowry, O. H., N. J. Rosebrough, A. L. Farr, and R. J. Randall. 1951. Protein measurement with the phenol reagent. *J. Biol. Chem.* 193:265–275.
18. Chen, P. S., Jr., T. Y. Taribara, and H. Warner. 1956. Microdetermination of phosphorus. *Anal. Chem.* 28:1756–1758.
19. Weibel, E. R., G. Losa, and R. P. Bolender. 1976. Stereological method for estimating relative membrane surface area in freeze-fracture preparations of subcellular fractions. *J. Microsc. (Oxf.)*. 107:225–266.
20. Scales, D., and G. Inesi. 1976. Assembly of ATPase protein in sarcoplasmic reticulum membranes. *Biophys. J.* 16:735–751.
21. Wang, C. T., A. Saito, and S. Fleischer. 1979. Correlation of ultrastructure of reconstituted sarcoplasmic reticulum membrane vesicles with variation in phospholipid to protein ratio. *J. Biol. Chem.* 254:9209–9219.
22. Klug, A., and J. E. Berger. 1964. An optical method for the analysis of periodicities in electron micrographs and some observations on the mechanism of negative staining. *J. Mol. Biol.* 10:565–569.
23. Taylor, C. A., and H. Lipson. 1965. Optical Transforms, Plate 1. *In* Optical Transforms. Cornell University Press, Ithaca, New York.
24. Frey, T. G., S. H. P. Chan, and G. Schatz. 1978. Structure and orientation of cytochrome c oxidase in crystalline membranes. *J. Biol. Chem.* 253:4389–4395.
25. Pringle, J. W. S. 1968. Mechano-chemical transformation in striated muscle. *In* Aspects of Cell Motility. P. L. Miller, editor. Cambridge University Press, Cambridge. 67–87.
26. Inesi, G. 1972. Active transport of calcium ion in sarcoplasmic reticulum membranes. *Annu. Rev. Biophys. Bioeng.* 1:191–210.
27. Watanabe, T., D. Lewis, R. Nakamoto, M. Kurzmack, C. Fronticelli, and G. Inesi. 1981. Modulation of calcium binding in sarcoplasmic reticulum adenosine triphosphatase. *Biochemistry*. 20:6617–6625.
28. Ikemoto, N., A. M. Garcia, Y. Kurobe, and T. L. Scott. 1981. Nonequivalent subunits in the calcium pump of sarcoplasmic reticulum. *J. Biol. Chem.* 256:8593–8601.
29. Coan, C., and S. Keating. 1982. Reactivity of sarcoplasmic reticulum adenosinetriphosphatase with iodoacetamide spin-label: evidence for two conformational states of the substrate binding site. *Biochemistry*. 21:3214–3220.
30. Saito, A., C. T. Wang, and S. Fleischer. 1978. Membrane asymmetry and enhanced ultrastructural detail of sarcoplasmic reticulum revealed with use of tannic acid. *J. Cell Biol.* 79:601–616.
31. Burkli, A., and R. J. Cherry. 1981. Rotational motion and flexibility of Ca^{2+}, Mg^{2+}-dependent adenosine 5'-triphosphatase in sarcoplasmic reticulum membranes. *Biochemistry*. 20:138–145.
32. Franzini-Armstrong, C. 1974. Freeze fracture of skeletal muscle from the tarantula spider. *J. Cell. Biol.* 61:501–513.
33. Franzini-Armstrong, C. 1975. Membrane particles and transmission at the triad. *Fed. Proc.* 34:1382–1389.
34. Franzini-Armstrong, C. 1980. Structure of sarcoplasmic reticulum. *Fed. Proc.* 39:2403–2409.
35. Crowe, L.M., and R. J. Baskin. 1978. Freeze fracture of intact sarcotubular membranes. *J. Ultrastruct. Res.* 62:147–154.
36. Rayns, D. G., C. E. Devine, and C. L. Sutherland. 1975. Freeze fracture studies of membrane systems in vertebrate muscle: striated muscle. *J. Ultrastruct. Res.* 50:306–321.
37. Bray, D. F., and D. G. Rayns. 1976. A comparative freeze-etch study of the sarcoplasmic reticulum of avian fast and slow muscle fibers. *J. Ultrastruct. Res.* 57:251–259.
38. Scales, D., R. Sabbadini, and G. Inesi. 1977. The involvement of sarcotubular membranes in genetic muscular dystrophy. *Biochim. Biophys. Acta.* 465:535–549.